Thickness of Cenozoic Deposits of Yucca Flat Inferred from Gravity Data, Nevada Test Site, Nevada

by G.A. Phelps[1], V.E. Langenheim[1], and R.C. Jachens[1]

Open-File Report 99-310

1999

This report is preliminary and has not been reviewed for conformity with U.S. Geological Survey editorial standards or with the North American Stratigraphic Code. Any use of trade, firm, or product names is for descriptive purposes only and does not imply endorsement by the U.S. Government.

Manuscript approved xxx

U.S. DEPARTMENT OF THE INTERIOR
U.S. GEOLOGICAL SURVEY

[1]Menlo Park, California

Abstract

The basin-basement contact for Yucca Flat was modeled using isostatic gravity data,

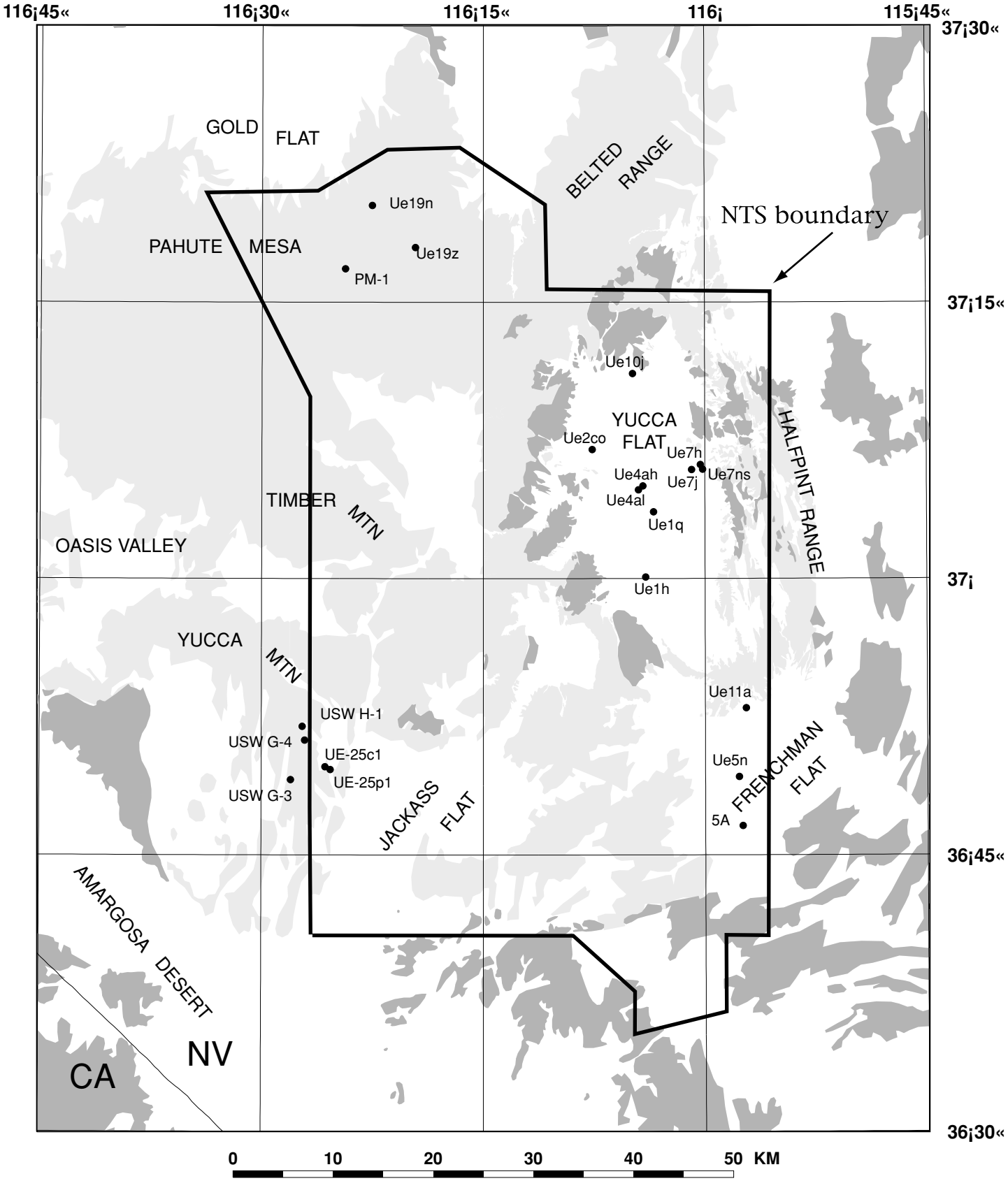

Figure 1. Map showing simplified geology of the Nevada Test Site region. White, Cenozoic alluvial deposits; light gray, Cenozoic volcanic rocks; dark gray, pre-Cenozoic rocks; black circles, well locations that contain borehole gravity measurements.

For the purposes of the gravity inversion we divide the geology into basement and basin fill units (fig. 2). We define basement as all pre-Cenozoic units and basin fill as Cenozoic units. Generally a large density contrast is observed between the two for the Basin and Range area (Jachens and Moring, 1990). Separating basement units from basin fill units on the surface allows us to distinguish gravity signals of basement rocks from gravity signals which contain both basement and basin fill components.

Further geologic constraints were provided by drill hole data. Wells which reached basement pinned the basement depth of the model at various points and served as important constraints for defining the gravitational signal of the basement rocks.

Gravity Data

Gravity data were taken from an existing dataset of gravity stations in the Nevada Test Site (Ponce, 1997). There are 9,883 stations in our study area (fig. 3). Of those, 401 gravity stations are on the basement rock surrounding Yucca Flat, and roughly 7,300 stations are on basin fill in Yucca Flat. The remainder are on basin fill surrounding Yucca Flat. The station spacing in Yucca Flat itself is dense, on the order of 200 m. Outside Yucca Flat the spacing ranges from 200 m to 2 km or more, with reasonably uniform coverage throughout the area. Gravity data were reduced using the Geodetic Reference System of 1967 (International Union of Geodesy and Geophysics, 1971) and referenced to the International Gravity Standardization Net 1971 gravity datum (Morelli, 1974, p. 18). Gravity data were reduced to complete Bouger gravity anomalies (Plouff, 1977) with a reduction density of 2.67 g/cm^3 by applying earth-tide, instrument drift, free-air, Bouger, latitude, curvature, and terrain corrections. An isostatic correction, following the method and parameters used by Jachens and Griscom (Jachens and Griscom, 1985), using a sea-level crustal thickness of 25 km (16 mi) based on seismic profiles, a crustal density above sea level of 2.67 g/cm^3, and a mantle-crust density contrast of 0.40 g/cm^3 was applied to the gravity data to remove the long-wavelength gravitational effect of isostatic compensation of the crust due to topographic loading. The resulting isostatic residual gravity data, or simply residual gravity data, are the primary data on which this study is based.

Figure 2. Map showing simplified geology of the Yucca Flat area, Nevada Test Site. See figure 1 for explanation of

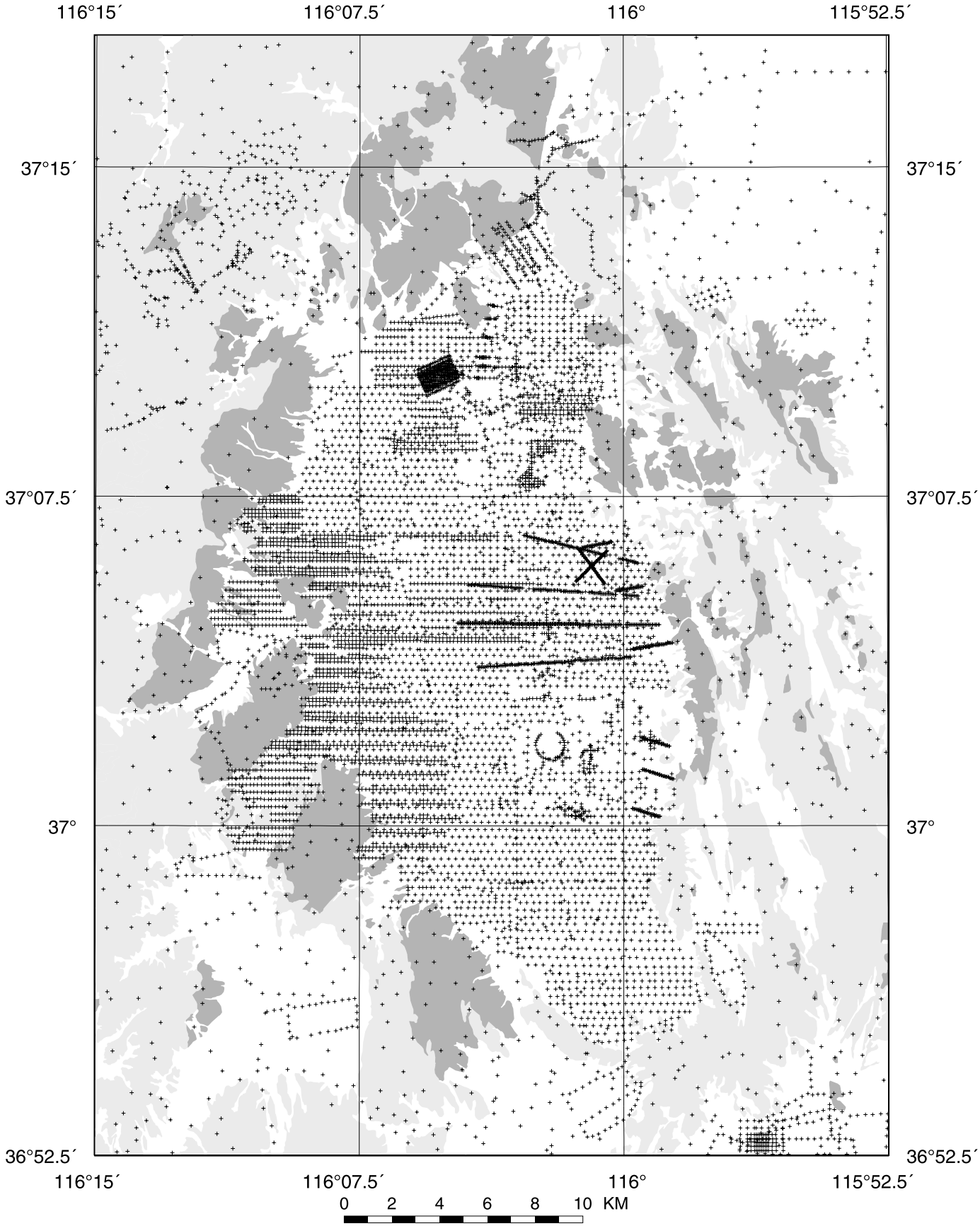

Figure 3. Map showing gravity stations used to model the depth to pre-Cenozoic basement beneath Yucca Flat. See figure 1 for explanation of the geology.

Apparent in the residual gravity field are incongruous data values, often seen as a single value higher or lower than surrounding values, showing as pits and spikes in figure 4a. In the northwest portion of the basin are a series of values from a particular survey that are anomalously higher than surrounding values, showing up as a waffle pattern in figure 4b. In Yucca Flat we used a modified version of the residual gravity data, one in which we removed erroneous data points. Anomalous gravity readings are common in large gravity datasets, and are generally produced by measurement or processing errors that are difficult to correct. These bad readings cause a spike or pit in the data that has a much shorter wavelength than that which could be produced by variations in depth to basement. The simplest solution is to delete the anomalous data points, provided the dataset is large enough and evenly distributed enough to justify it. Yucca Flat has 9,883 total data points, of which we deleted 261, resulting in a dataset of 9,622 data points. The deleted points are shown in blue in figure 4a and 4b. A table of the values and station identification codes of points deleted is contained in an ASCII file in the digital dataset for this report.

Drill Hole Data and Physical Properties

Drill-hole information for 1,205 wells in the Nevada Test Site area (992 in Yucca Flat), originally compiled by Van Williams of the U.S. Geological Survey, was obtained in the form of a spatial database (R. Wahl, unpub. database, 1998). One hundred seventy-nine of the wells in the database in Yucca Flat reached basement (fig. 2), distributed primarily in the northeastern part of the basin. Twenty-one wells in the Nevada Test Site region have separately published borehole gravity information for at least part of the total well depth (Healey 1967a, b; Healey and others, 1984, 1986; Kososki and others, 1987; Robbins and others 1982, 1983; Schmoker and others, 1978), nine of which are in Yucca Flat (fig. 1).

An estimate of the density of the basement rocks and of the density contrast between the basement and the overlying rocks are required for estimating basement depth using gravity. Previous works which use gravity to estimate the basement depth in Yucca Flat use a basement density value of 2.67 g/cm^3 and a constant density contrast of -0.70 g/cm^3 (Healey, 1968), and a basement density value of 2.50 g/cm^3 and a constant density contrast of -0.70 g/cm^3 (Ferguson and others, 1988). While both studies recognized lateral and vertical density variations in the basin fill, neither found enough consistency to justify a more complicated density model. Borehole gravity smoothes the effects of local variations in density and yields a more generalized measure of density than other

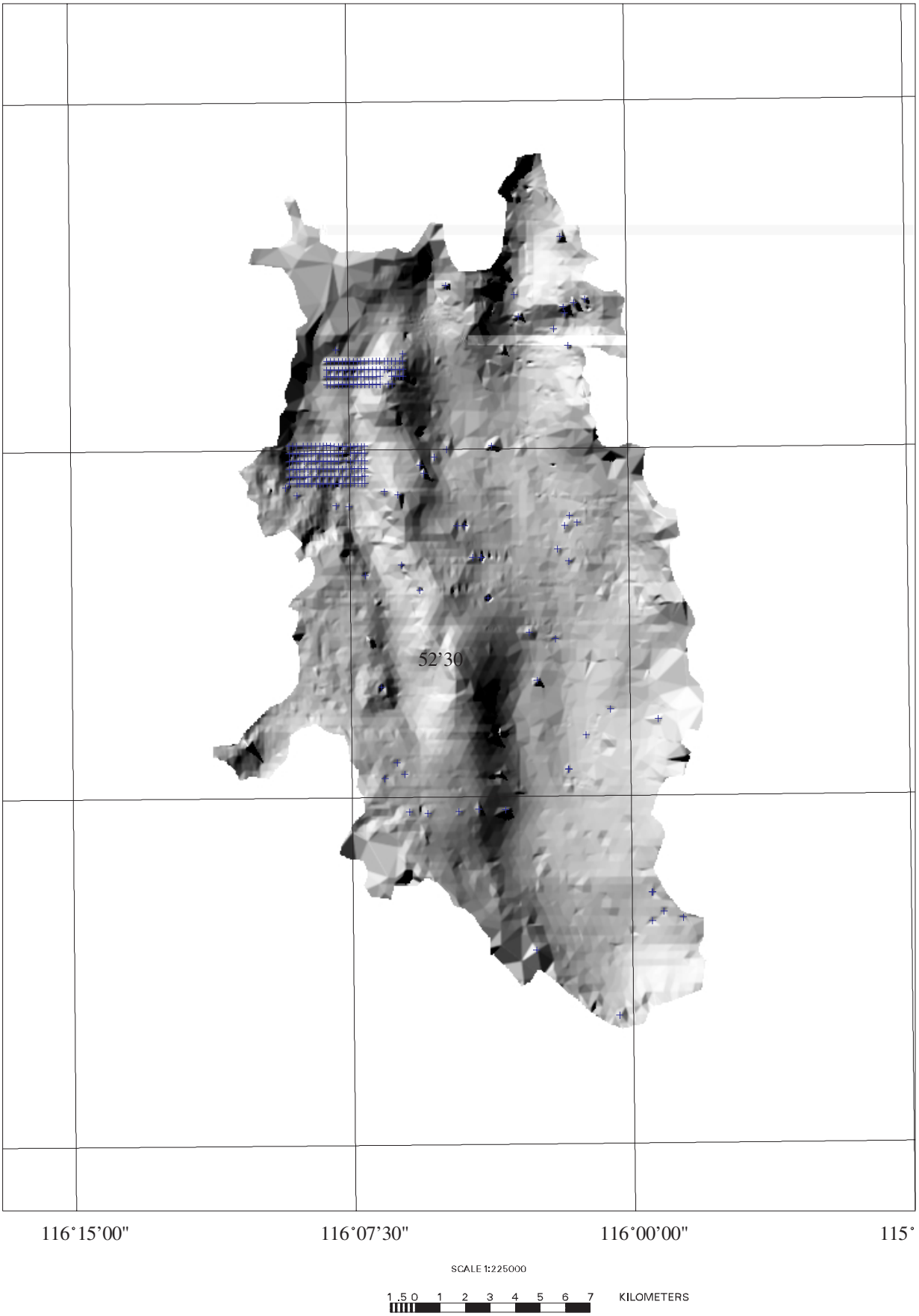

Figure 4a. Shaded relief map of isostatic residual gravity for Yucca Flat and vicinity. Crosses, points deleted from original dataset.

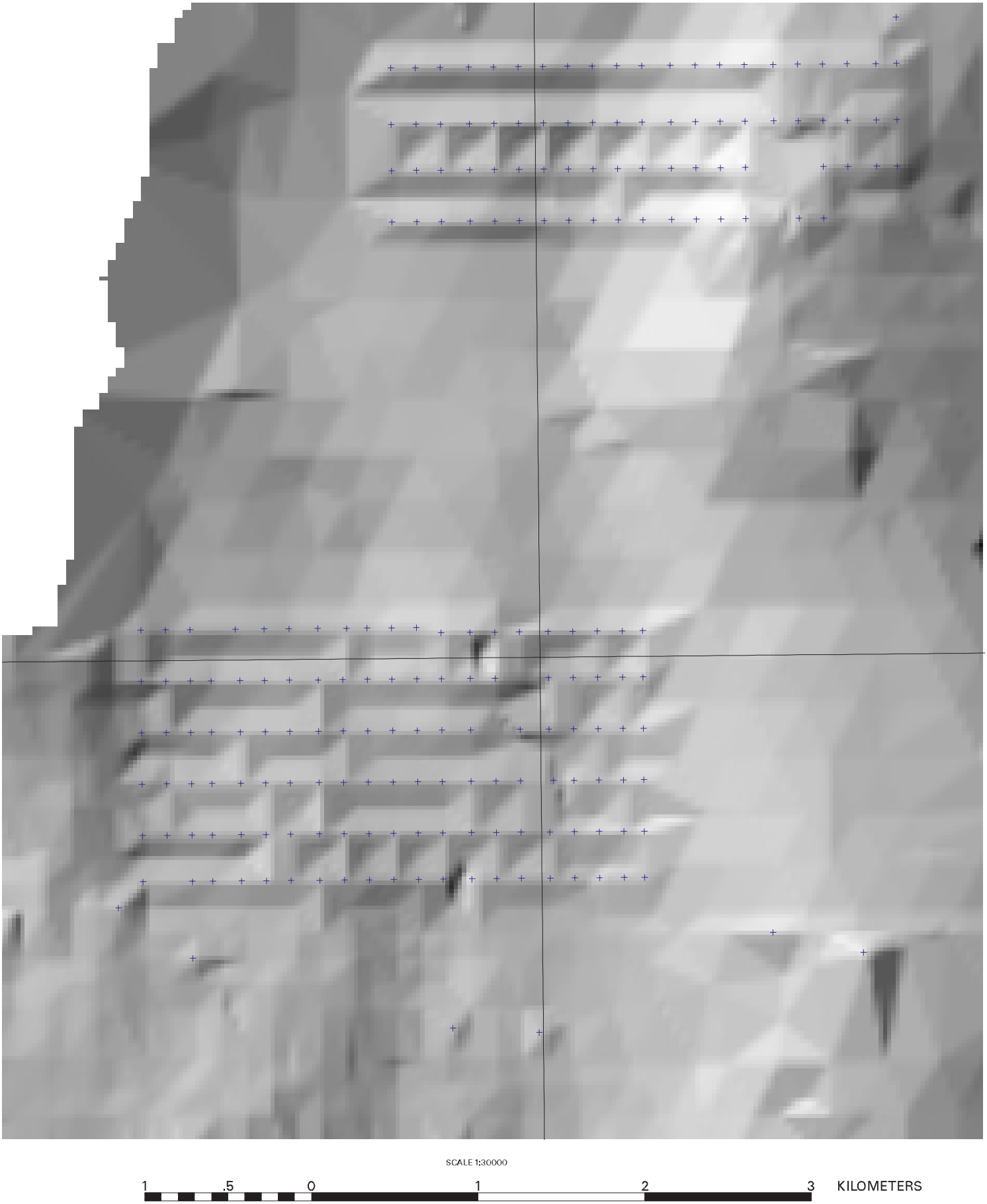

Figure 4b. Detailed shaded relief map of isostatic residual gravity for Yucca Flat, showing the "waffle" pattern. Crosses, points deleted from original dataset.

methods (density logs and rock sample measurements, for example). We feel the borehole gravity data from Yucca Flat allow us to use the following density model:

1) use an average basement value of 2.67 g/cm^3

2) use a linear function for the density contrast in the basin fill

The median density of the basement rocks is 2.65 g/cm^3, and the mean is 2.60 g/cm^3. Because the data are not normally distributed the median is a more robust indicator of the center of the distribution than is the mean. This value is very close to the 2.67 g/cm^3 value used for the average basement density value for the Basin and Range (Jachens and Moring, 1990) and the value used to reduce the gravity data. The borehole gravity data are therefore consistent with previous results of Basin and Range basement density values. We feel the density data do not warrant a re-reduction of the gravity data.

The density-depth relationship, along with the simple linear regression fit, is shown in figure 5 (dashed line). It is a linear model of the form

$\rho = .0006z + 1.76$ where z = depth, in meters, and ρ = density, in g/cm^3

Note that the low slope is a function of non-standardized variables and does not indicate a low level of significance. The fit is significant at the one percent level, with a multiple R-square of 0.30. The regression diagnostics are shown in figure 6, demonstrating the assumptions of a linear relationship are met. Figure 6a shows the residuals are evenly distributed along the regression line. Figure 6b shows the residuals are normally distributed (with slight thinning at the tails). Figure 6c is the residual-fit plot, a measure of the variation accounted for in the fit against the variation left in the residuals. As the residual-fit plot shows, there is still a substantial amount of information not explained by the linear model. The densities of the basin fill units do show a definite trend with depth in Yucca Flat, according to the borehole gravity data. Though much variation exists in the data, a linear model does explain 30% of the trend and is an improvement over the use of a single density value for all basin fill.

Recent work by the authors has shown the model can be improved by separating the data into two populations, one associated with Quaternary alluvium and the other associated with Tertiary volcanic rocks. A moving window regression curve (known as a "loess" curve, for LOcally wEighted regreSSion; loess curves and residual-fit plots are discussed in Cleveland, 1993) was fitted to the dataset (solid line in fig. 5). The curve flattens at shallow depths, a consequence of the influence of the Quaternary units. These Quaternary units cause the simple linear regression slope to be smaller than that representing the volcanic rocks alone.

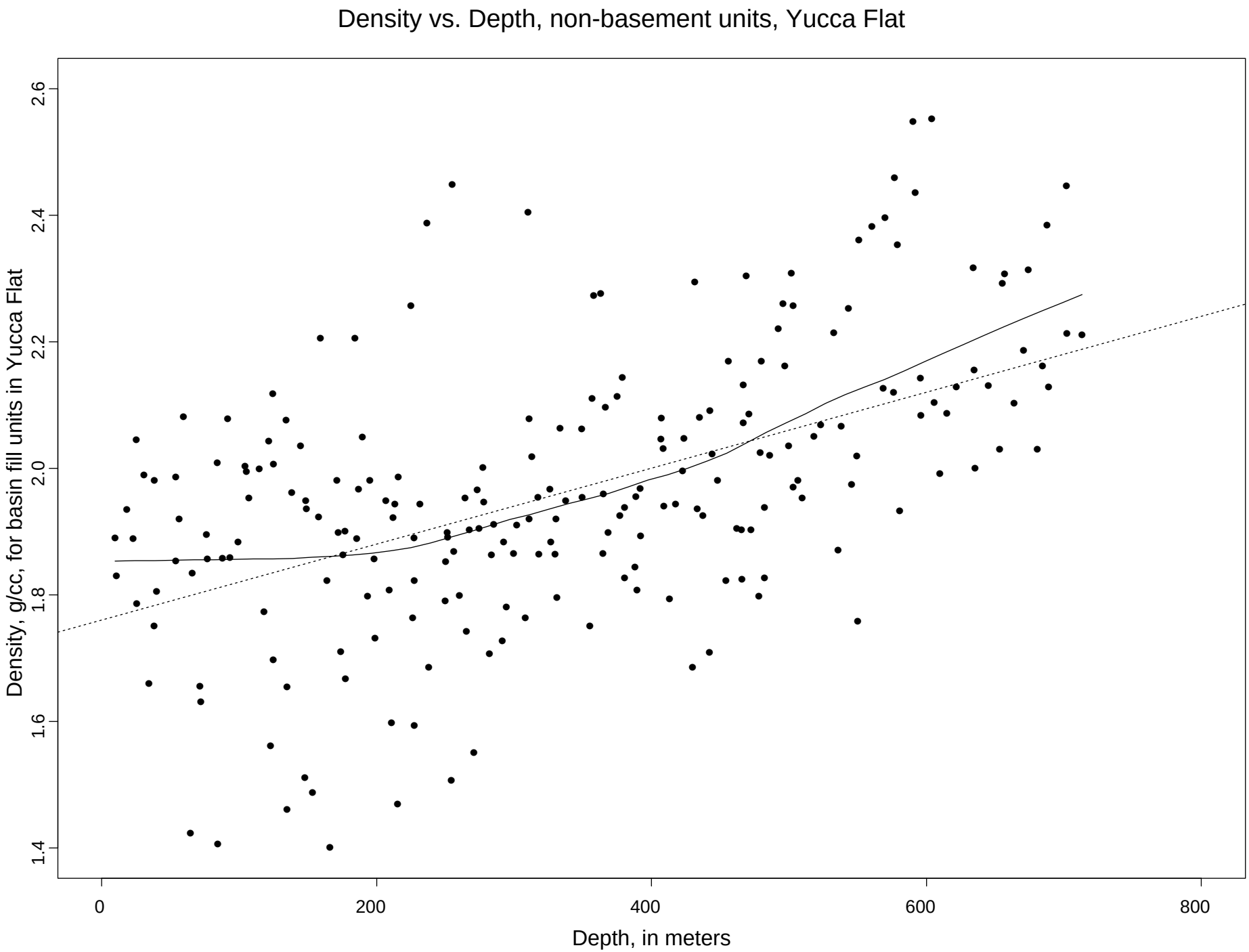

Figure 5. Linear regression (dashed line) fitted through borehole gravity data points, used to model density vs. depth. Solid line is a moving-window linear regression, included for comparison.

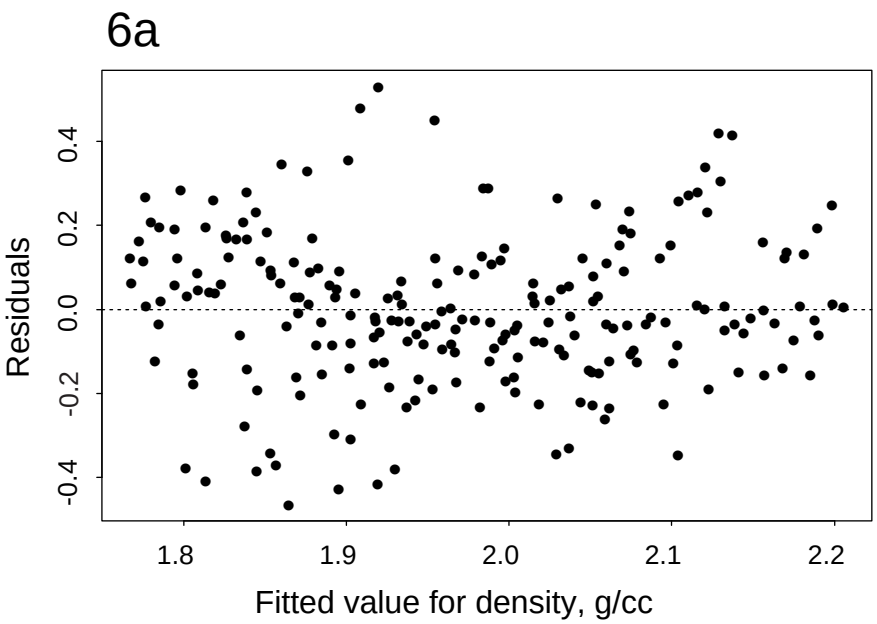

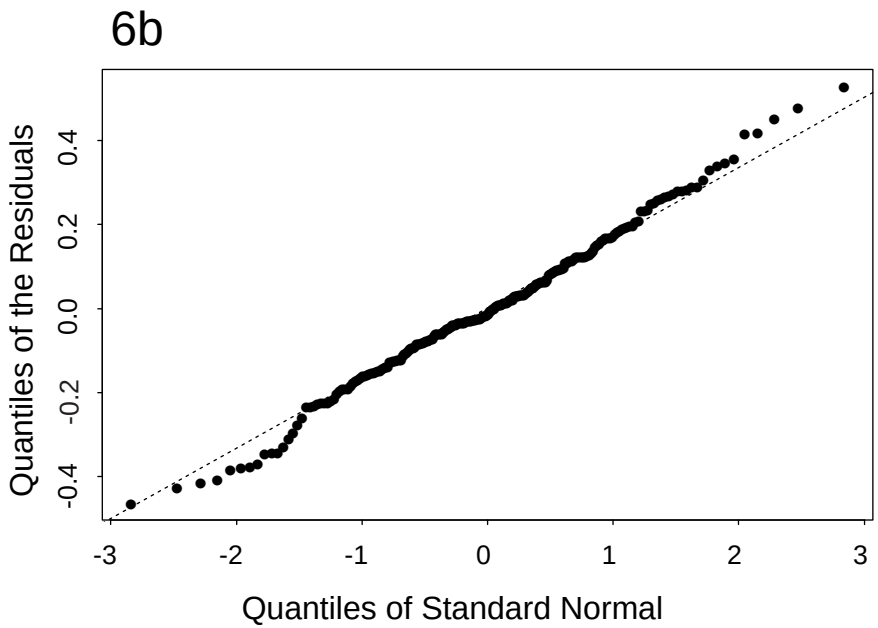

Figure 6a. The residuals should be evenly distributed about the fitted regression line. This diagram is meant to show whether the residuals are evenlydistributed about the line or show evidence of preferred clumping or systematic shifts of the data along the fit. This diagram shows that the residuals are reasonably evenly distributed.

Figure 6b. Quantiles are a ranking of the data from lowest to highest, normalized to one. An individual quantile value is called the f-quantile or f-value (e.g. the 0.5 quantile, the data point having an f-value of 0.5, is the median). A quantile-quantile plot shows the ranking of one set of ranked data against another. If the distributions are the same the data points will plot along a straight line. In this case the quantiles of the residuals from the linear regression fit are compared with the quantiles of a standard normal distribution. If the residuals were exactly normally distributed the data points would plot along the dashed line. The axes show the residual values at a given quantile against the standard deviation values of the standard normal distribution at a given quantile, instead of f-values, because they are more meaningful. The residuals are normally distributed out to about 1.5 standard deviations, after that showing slight leptokurtosis.

Figures 6a and 6b. Diagnostic plots for the linear model of density vs. depth, shown in figure 5.

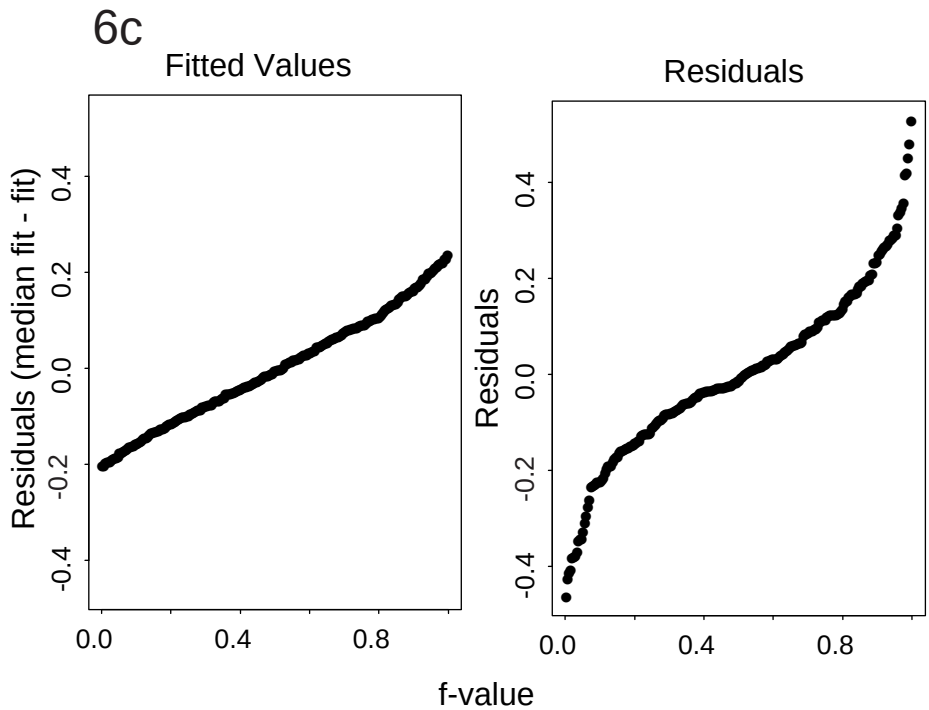

Figure 6c. Residual Fit plots are an attempt to look at the variation in the data explained by the regression fit compared to the variation still present in the data.

The diagram on the left shows the residuals of the fit (the mean value for the regression line fit minus the value for the fit at a particular location along the regression line) against the f-value (see figure 6b).

The diagram on the right shows the actual residuals from the regression (fit minus the data value for each data point) against the f-value.

Ideally the plot on the left will show a much greater range than the plot on the right, indicating that the fit explains much more of the variation in the data than is left in the residuals. This is not the case here. There is still a substantial amount of variation left in the data after we apply the fit, indicating that, in general, the linear model does a fairly poor job of explaining the variation in density with depth. If we were trying to model the density at a specific depth in the basin (for drilling purposes, for example) this would be a poor choice of models. However, in our case we are modeling a general trend across the basin and are simply looking for an improvement over a simple mean value. For this purpose the model is acceptable, since it accounts for far more variation in the data (30% according to the fit) than does a single average value.

Pooling the data from the other twelve borehole gravity logs creates a dataset with a large proportional effect (the data show extreme variability at the surface, diminishing significantly as depth increases). This indicates that a density relationship with depth in the other wells is not as clear as in Yucca Flat. The other data are from wells in Pahute Mesa, Yucca Mountain, and the western edge of Frenchman Flat, where geological differences from site to site may overwhelm any systematic change of density with depth.

Gravity Anomalies

Figure 7a shows a residual gravity low over Yucca Flat, with a prominent relative high trending N-S on the west side of the valley. The residual gravity field suggests a basin divided by a ridge, deepest east of the ridge, somewhat shallower to the west. The structure suggests a horst separating two grabens. In general, gravity values over the basement are high relative to those over the basin.

Variations in the residual gravity field over the basin are the combined result of variations in the near-surface basement gravity plus the basin fill gravity. To understand the topographic basement surface below Yucca Flat one must separate the gravity signal due to variations in the basement from those due to variations in the basin fill .

Depth to Basement

Method

The method used in this study to find the depth to basement based on the residual gravity field is an updated version of a method developed by Jachens and Moring (1990) that incorporates drillhole data (Bruce Chuchel, U.S. Geological Survey, written commun., 1996). Necessary inputs to the method are knowledge of the residual gravity field, of the exposed geology, and of the variation of density with increasing depth within the basin deposits. Basement density is assumed to be constant at 2.67 g/cc. Although vertical variations in density within the basement may be present, for example from a dense metamorphic part of the stratigraphic section at depth, they will not affect the depth determination unless they also vary laterally within the study area. In that case, anomalies due to basement density variations will be contained in the *basement gravity* field, another byproduct of the depth determination procedure (see below). Data from drill holes that penetrate basement rock and other geophysical constraints on depth to basement (e.g. seismic, or electrical soundings) can also be input into the model and provide useful constraints to the method as well as tests of the results.

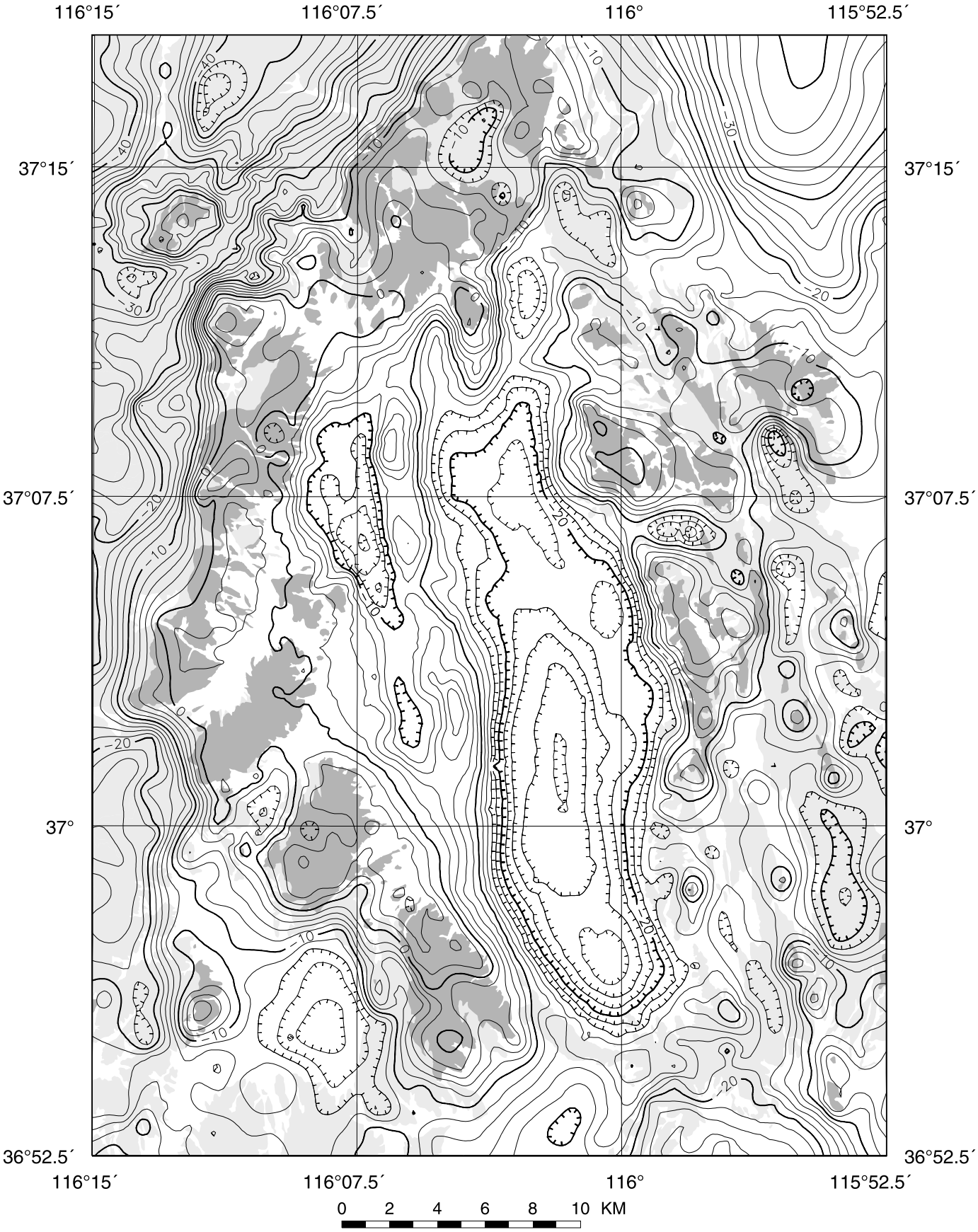

Figure 7a. Map showing isostatic residual gravity of the Yucca Flat area. Contour interval is 2 mGal. See figure 1 for explanation of geology.

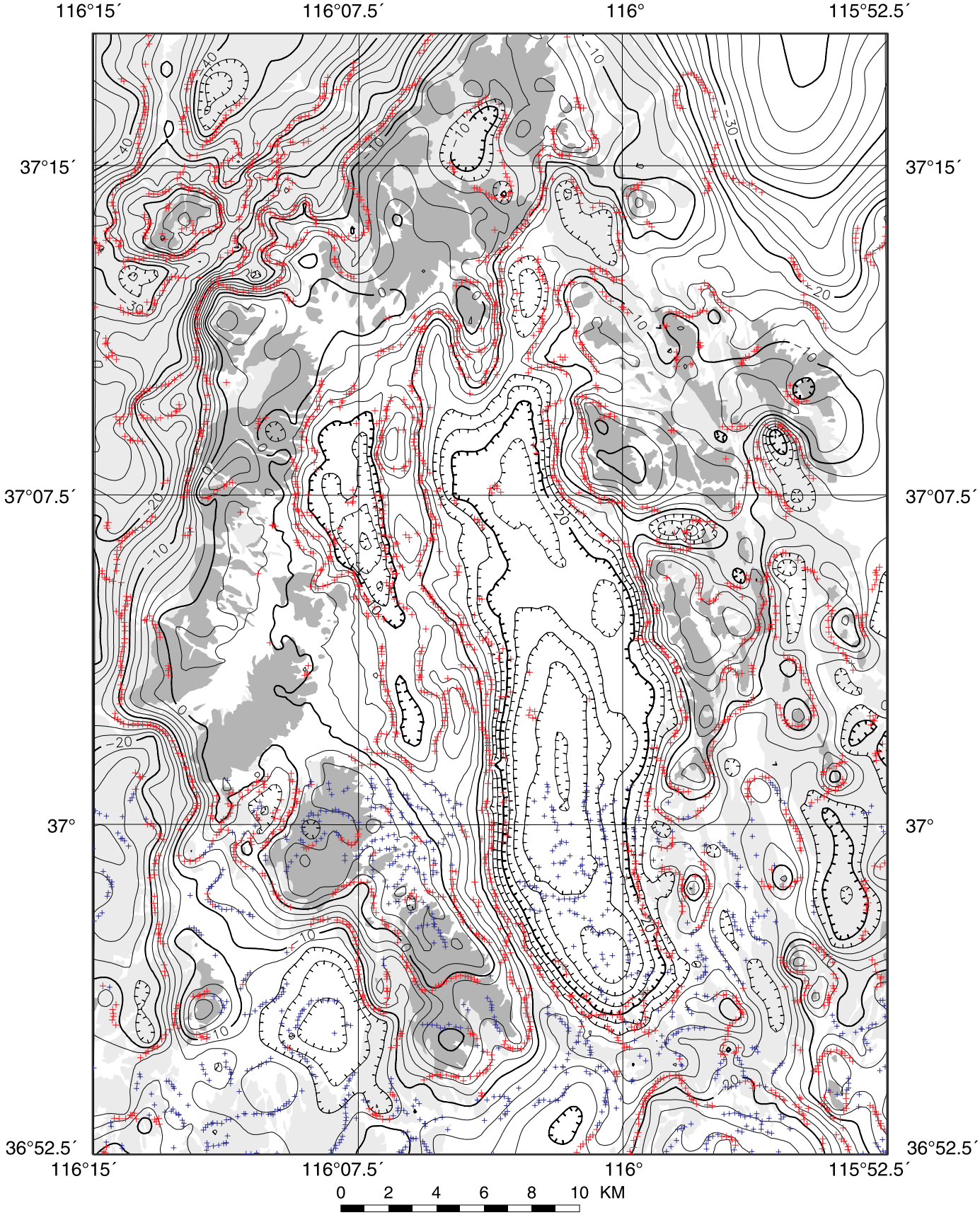

Figure 7b. Map showing isostatic residual gravity of the Yucca Flat area with maximum horizontal gradient points overlain. Red crosses are points above the average value, blue crosses are those below. Contour interval of the isostatic gravity is 2 mGal. Shaded areas indicate basement outcrops.

The residual gravity data (9,622 scattered data points mentioned in the section Gravity Data) were converted to a raster dataset with a 200 m cell size. This was used as the residual gravity grid input to the model.

The surface geology was separated into two groups, basement and basin fill, and converted from a vector dataset to a raster dataset with a 200 m cell size. This was used as the geology grid input to the model, and allows the model to distinguish between residual gravity values which are on basement and those that are on basin fill.

The variation of density with depth within the basin deposits was separated into five layers which varied with depth according to the linear density function described previously: 0-200 m was 1.82 g/cm^3, 200-400 m was 1.94 g/cm^3, 400-600 m was 2.06 g/cm^3, 600-800 m was 2.18 g/cm^3, and 800 m and greater was 2.30 g/cm^3. Although the last value extends the regression equation slightly beyond the data, the value of 2.30 is reasonable because it is within the upper range of the data. The median value of the lowest Tertiary unit in the stratigraphic section (thus more likely to occur at depth) for depths below 500 m is 2.30 g/cm^3, which helps support the validity of the assumptions (based on the borehole gravity readings of the nine wells in Yucca Flat).

The depth to basement method attempts to separate the residual gravity field into two components: a *basement gravity* component caused by variation of density within the basement, and a *basin gravity* component caused by variations in thickness of the basin fill. The *basin gravity* component is the difference between the residual gravity field and the *basement gravity* field as estimated from gravity observations made on outcrops of basement rock and at the sites of wells that penetrate the basement. The *basin gravity* component is inverted to yield the thickness of basin deposits based on the model density-depth function that characterizes these deposits. It is significant that the gravity is separated into two components. Using our method we are able to obtain a *basement gravity* field constrained by well data which contains information about the density of the basement rocks. The basement field gives us a glimpse of the geology of the basement beyond what the well data alone can tell us.

The accuracy of the initial inversion is complicated because the *basement gravity* field varies due to density variations within the basement. The inversion presented here does not take into account lateral variations in the density distribution of the basin deposits. To accommodate the variations in the *basement gravity* field, a first approximation of the *basement gravity* field is determined by interpolating a smooth surface through all gravity values measured on basement outcrops. The *basin gravity* is then the difference between the observed gravity field on the original map and the first approximation of the *basement gravity* field and is used to calculate the first approximation of the thickness of basin

deposits. The thickness is forced to zero where basement rocks are exposed. This first approximation of the *basement gravity* is too low near the basin edges because of proximity of the low-density deposits to the basement stations. The *basement gravity* station values are "corrected" for the effects of the low-density deposits (the effects are calculated directly from the first approximation of the thickness of the basin deposits) and a second approximation of the *basement gravity* field is made by interpolating a smooth surface through the corrected *basement gravity* observations. This leads to an improved estimate of the *basin gravity* field, an improved depth to basement, and a new correction to the *basement gravity* values. This procedure is repeated until successive iterations produce no significant changes in the *basement gravity* field, typically about 5 iterations.

Well data provides an important constraint to the model depth. As the model iterates, it assumes the difference between the modeled *basement gravity* and isostatic residual gravity is due solely to the effect of the basin sediments. Therefore, the method will overestimate the depth of the basin if the true gravity of the basement is lower than the model, and underestimate the depth of the basin if the true gravity of the basement is higher than the model. However, we can add the additional information from well data, which pins the basement depth and therefore the basin fill gravity component. If we compare the calculated thickness of the basin to the actual thickness at well sites we can add the excess gravity signal back into the basement gravity signal, thus refining the*basement gravity* component.

The model is not forced to conform exactly to the well depths because the model is a fitted surface, but it usually follows the well depths very closely. Problems can occur, however, when information is apparently contradictory. One example is two wells separated by a horizontal distance closer than the horizontal resolution of the data (e.g. they fall within the same grid cell) which have very different depths, as might occur across a fault. In this case the model cannot accommodate the data from both wells. The closest data point is used if there are data points within 0.5 cell widths. If no data points are that close, a weight average of data points within 0.75 cell widths is used.

Results

Figures 8, 9a and 9b show the results of the method given a 200 m residual gravity grid, a geology grid separated into basement and basin fill values, the linear density-depth function, and the 179 wells which reached basement. Figure 8 is an isopach map of the basin fill. Figure 9a is a shaded relief map of the topography of the study area with the basin fill stripped away and the resulting basement surface colored and figure 9b adds to

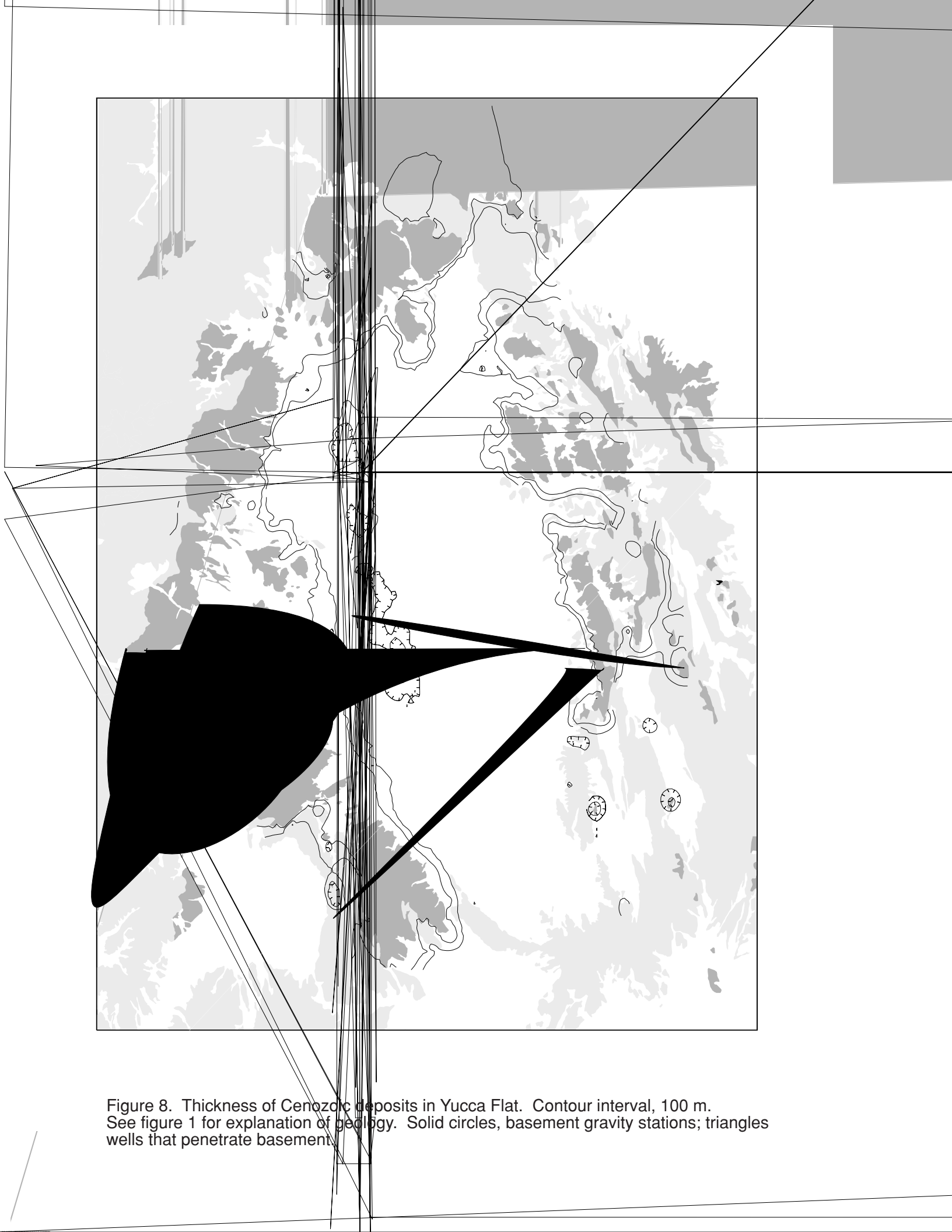

Figure 8. Thickness of Cenozoic deposits in Yucca Flat. Contour interval, 100 m. See figure 1 for explanation of geology. Solid circles, basement gravity stations; triangles wells that penetrate basement.

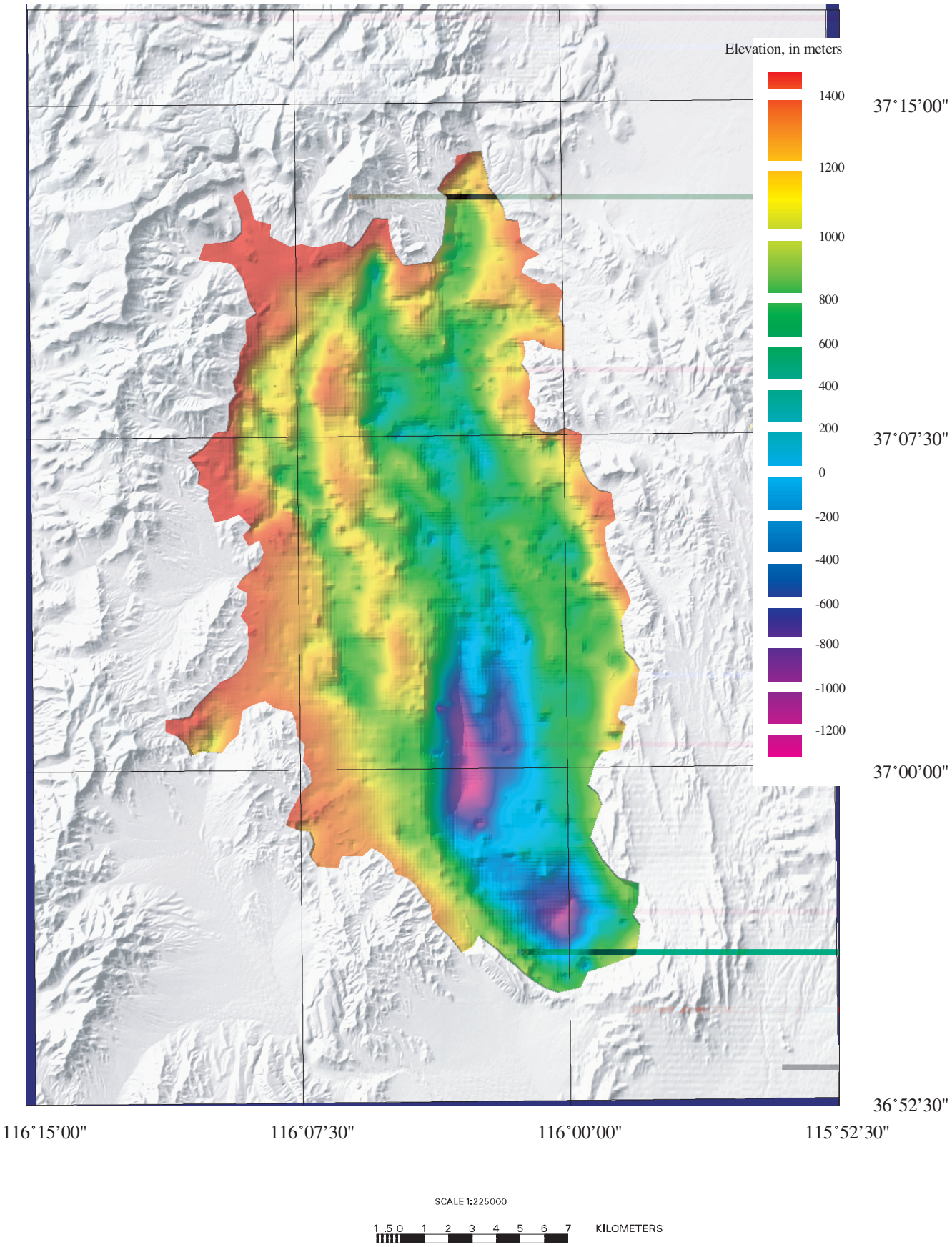

Figure 9a. Shaded relief map of Yucca Flat area with Cenozoic deposits of the Yucca Flat basin (colored area) stripped away.

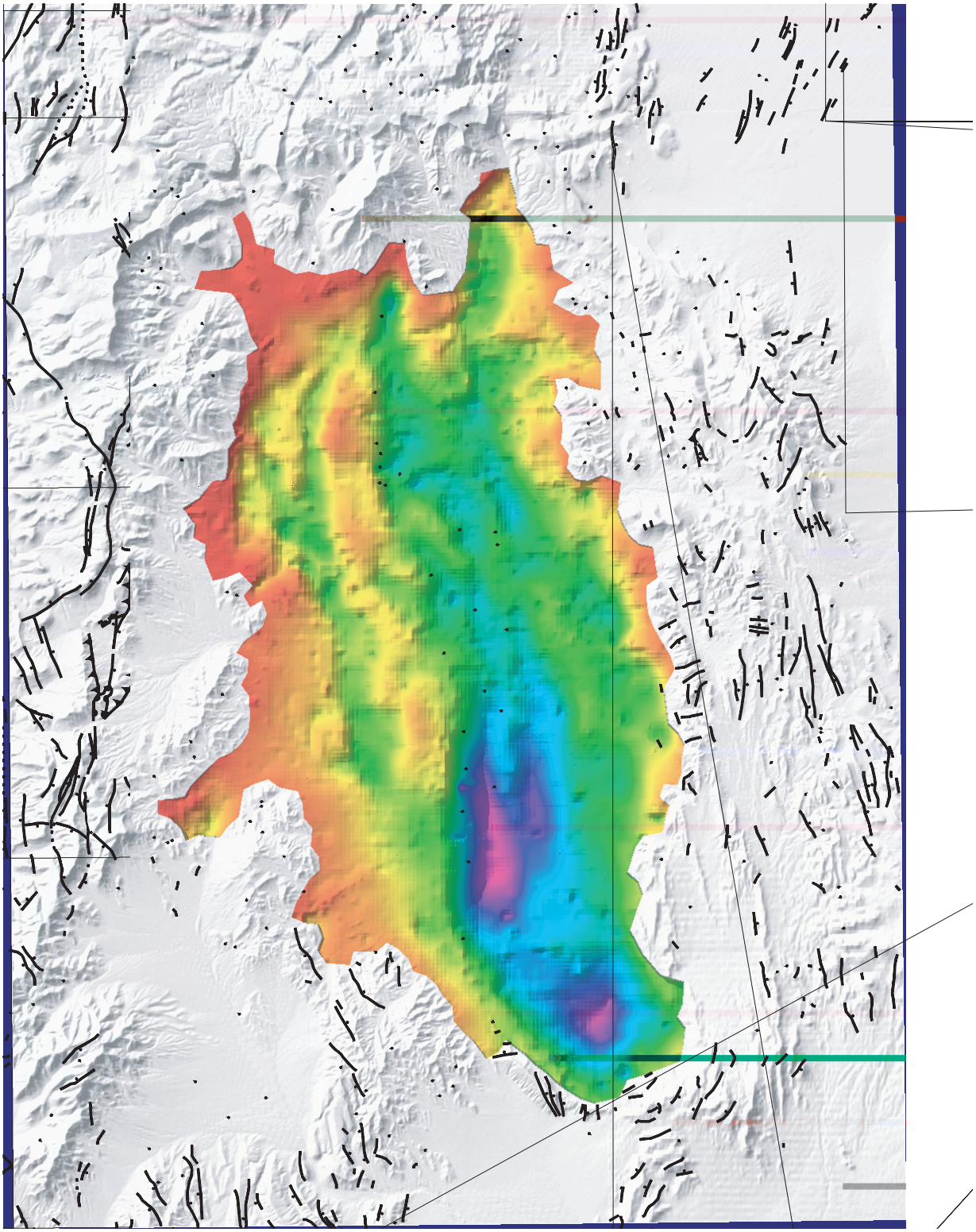

that the mapped surface faults and maximum horizontal gradient points from the residual gravity.

The difference between the actual depth and the model depth for wells that reach basement is shown in figure 10. As can be seen, the model conforms to known basement depths, in most cases to within 20 m. Anomalous wells are labeled with their identification code. In all cases these anomalous wells have a neighboring well within 120 m (about half the cell size of the model) whose depth is close to that of the model. In two cases another well with a different depth is co-located with the first well, indicating a contradiction in the dataset.

Figure 11 compares the model depth with the 813 wells in Yucca Flat which did not reach basement, and hence represent points of minimum depth to basement and an independent test of the model. Points above the zero line represent wells which do not reach basement and are deeper than the predicted depth. Only nine wells are deeper than the predicted model, and only one is greater than 50 m different. Well UE4aHTH, at 922 m depth, is 150 m deeper than the predicted model. It is located roughly in the center of the basin between the Carpetbag fault and the Yucca fault. It is surrounded by several wells which reached basement, in roughly a 1 km circle. Wells to the north and south which reach basement have values in excess of 900 m and are located in the trough between the two faults, while wells to the east and west have values from 600 m to 800 m and are located on higher areas beside the trough. The model inserts a slightly raised saddle in the trough at the location of well UE4aHTH, probably a function of the minimum curvature algorithm used to interpolate values between data points.

The model basement surface conforms well to the basement data used as constraints, and passes, in almost all cases, the independent test of 813 wells that do not reach basement. Therefore, the model basement surface seems to be a very reasonable approximation of the true surface.

Discussion

There are two reasons for re-examining the gravity data in Yucca Flat: first, to try to improve the estimates of depth to basement using a new technique, and second, by using this method, to look at the gravity signature of the basement to attempt to learn more about the geology of the basement. Both support the objective: to search for and identify structures that influence the movement of ground water.

The results from the "best" model are shown in figure 9a as a shaded relief map of topography with the Yucca Flat basin sediments stripped away. Figure 9b adds

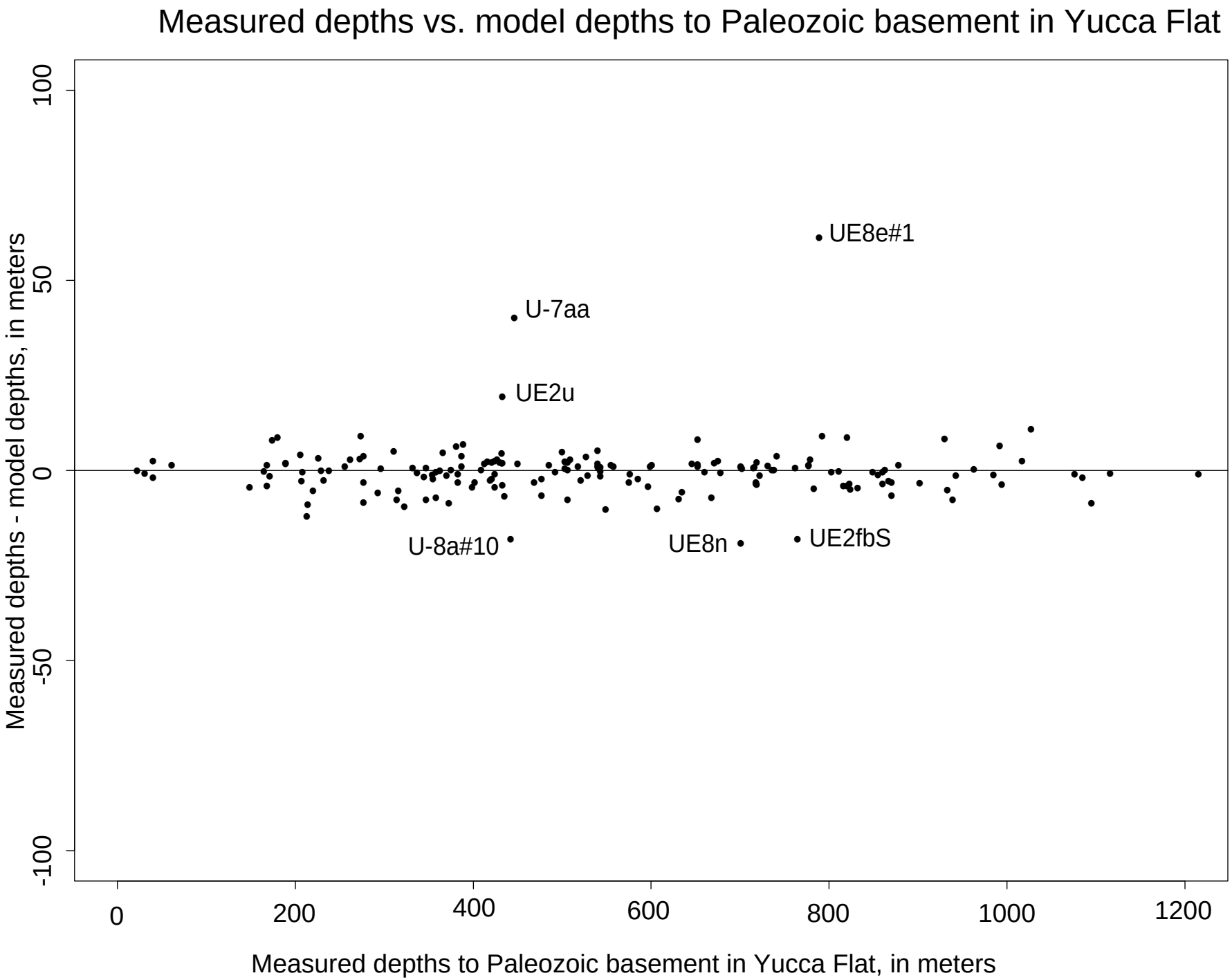

Figure 10. Plot of measured depths to pre-Cenozoic basement vs. measured depths minus model depths (residuals), for the 179 wells which modeled basement in Yucca Flat.

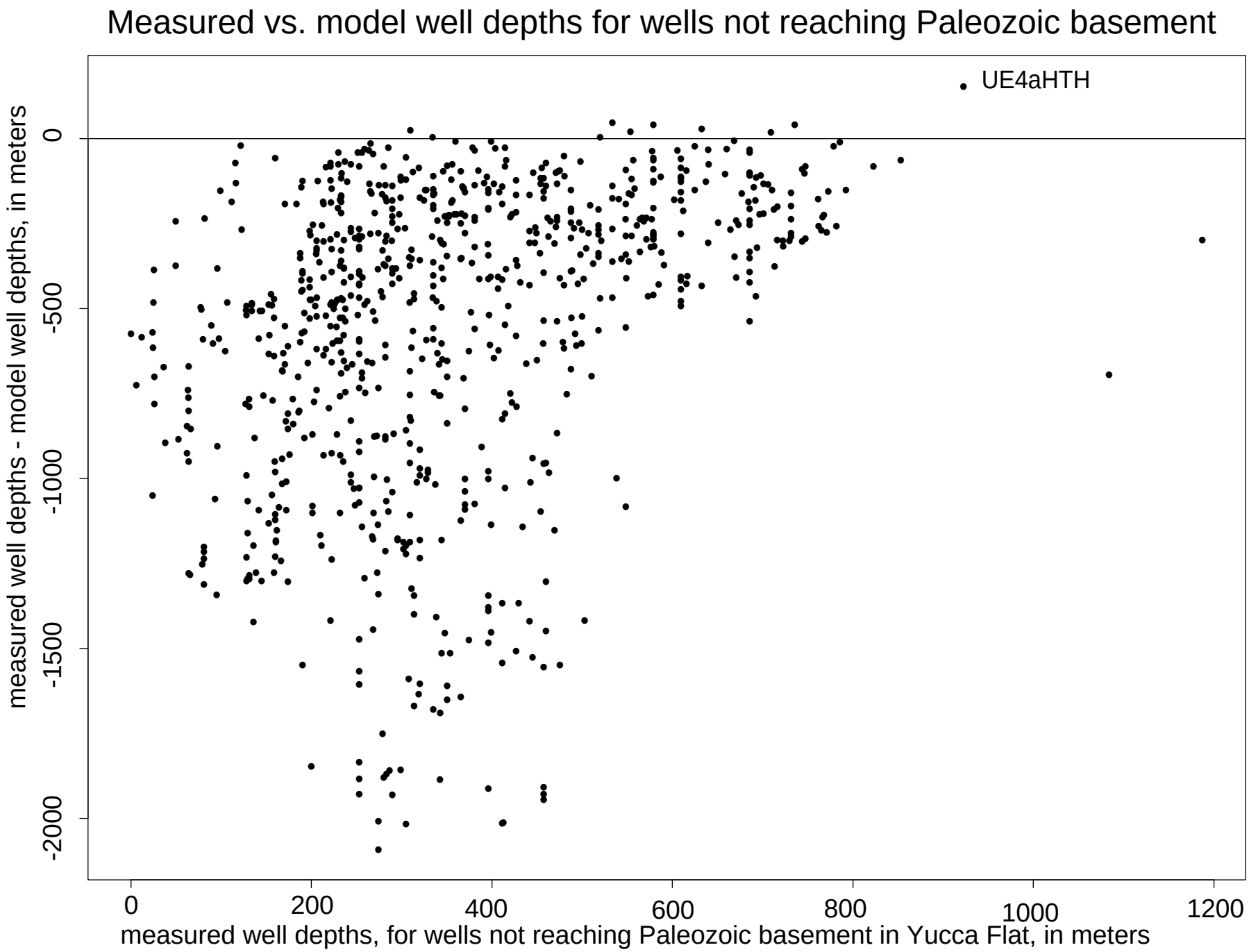

Figure 11. Measured well depths vs. measured well depths minus model basement depths, for wells not reaching basement in Yucca Flat. Wells above the zero line indicate where the model is too shallow (wells not reaching basement are deeper than predicted). The largest outlier is identified by its well identification number.

maximum-horizontal-gradient points and drapes faults from the geologic map (Wahl and others, 1997) onto the model basement surface.

The model differs from the previous model published by Ferguson and others (1988) and Klima (1990). The differences arise, in part, from presentation. Improved technology has made commonplace displays such as colored shaded relief maps, which present topography in a way that is easy to visualize. Also, we had the benefit of greater well control (179 vs. 90 wells for Ferguson and 151 wells for Klima) which constrained basement values. It is difficult to compare a contoured paper figure with a digital surface model, but gross features can be compared. Visually comparing them, both previous models and our model predict, to a first order, a similar basin shape. The models of Ferguson and Klima are similar in shape and magnitude, but the major basin features, the north-south trending horst and graben features, are more apparent in Ferguson's model, whereas the local highs and lows in Klima's model appear as more isolated features. Our model differs in magnitude from both previous models, predicting a thicker basin fill in the southern part of the basin where there is no well control. In particular, our model predicts a basement roughly 2.5 km deep in the southern part of Yucca Flat, whereas Ferguson and Klima predict roughly half of that. Similar to Ferguson's model, our model produces a linear structure to the major basin features. In addition, our model significantly increases the resolution of the modeled basement topography. Smaller-scale offsets, such as the offset created by the Yucca fault, are present in our model and absent, at the 100 m contour interval resolution, from both previous models. Another very subtle feature in our model that is not seen in the previous models is a possible stream channel along the west margin of the basin (approximately latitude 37° 05').

In addition to the isostatic gravity values one can also examine the gradient of the gravity field. Local maximum-horizontal-gradient points occur over edges for near vertical and shallow sources (Blakely and Simpson, 1986). As the first two factors diminish and the depth increases the maxima become less prominent. Maximum gradient points are useful for delineating shallow (less than 10 km), near vertical lithologic boundaries, which are commonly faults. We subdivided the points into two groups: those greater than the average value and those less than the average value. These help highlight primary and secondary features, and are shown in figure 7b.

In Yucca Flat the major surface faults lie along points of maximum horizontal gradient. The Carpetbag fault is the major basin-controlling fault, coinciding with a significant density boundary. Note that the trace of the maximum density contrast deviates from the mapped surface fault at about the midpoint, indicating a significant horizontal displacement of the basement feature relative to the surface feature.

The Yucca fault, though impressively exposed on the surface, is less impressive in the gravity data than the major features indicated in the gravity maxima. It is a feature with comparatively small vertical offset in the basement topography. Also note that the offset lies to the east of the mapped fault, which is consistent with the eastward dip of the fault. Based on the displacement of the basement feature, which moves progressively eastward from the mapped surface fault as one traces the fault southward, the dip decreases to the south.

In general, western edges of grabens are marked by higher-amplitude gravity gradients, suggesting faults with greater offsets and an eastward-dipping regional pattern, consistent with the geologic interpretation. Alternately, larger gravity gradients could be caused by variations in the density of the basement rocks along older faults. Available well control suggests the former.

The basement gravity field is shown in figure 12. The major features in the *basement gravity* are a large gravity high in the southwestern part of the basin and higher gravity values along the western side of the basin than on the eastern side, with the change occurring along the trend of the Carpetbag and Yucca Faults. These suggest changes in density in the basement rocks and could be used to help constrain basement lithology, especially in areas of little or no well control.

Precautions on using the gridded dataset

The digital dataset of the depth to a basement in Yucca Flat accompanying this report was created using in-house software which interpolates a surface between scattered data points using a minimum curvature algorithm (Webring, 1981). This algorithm is well suited for potential field datasets because, like potential fields, it yields continuous surfaces with continuous first derivatives. The dataset has a 200 m cell resolution. Values between cell center locations can be estimated by fitting a surface to the set of gridded data points, a capability of many commercial software packages. However, the value at a random location between data points is sensitive to the method of interpolation. Comparisons at the well locations shown in figure 2 between the estimated depth using the in-house minimum curvature algorithm and the estimated depth using bilinear interpolations are shown in figure 13. As the figure shows, the differences can be on the order of 100 m or greater for a 200 m cell resolution. This result is greater than all but one of the model depths vs. actual depths based on the well data (well UE4aHTH has a 150 m mismatch). Even with a resolution as fine as 200 m significant error can be introduced to any further analysis simply by using a different surface interpolation

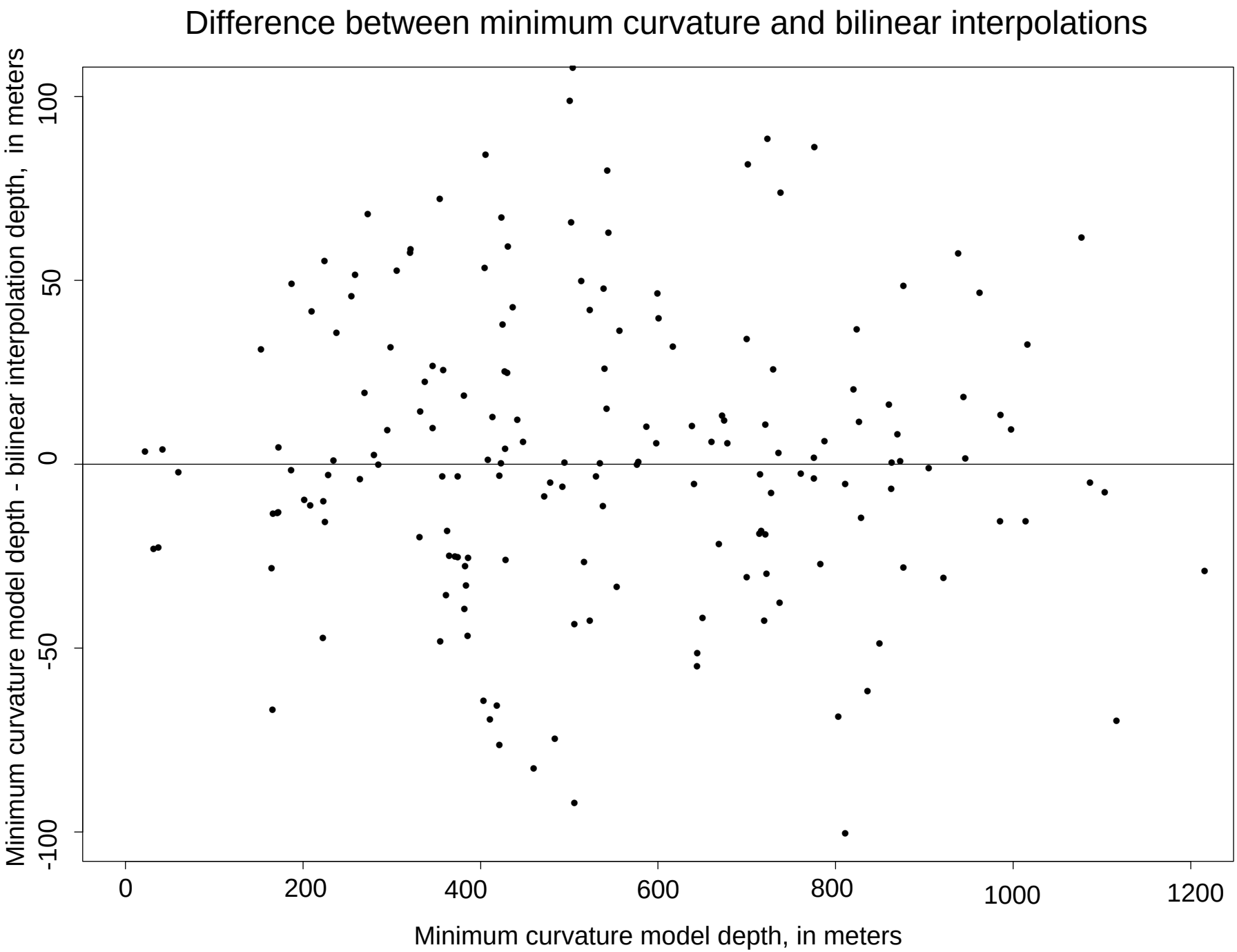

Figure 13. Difference between depths interpolated using minimum curvature method and depths interpolated using bilinear method. Points are wells which reached basement in Yucca Flat (shown in figure 2).

algorithm. We recommend fitting a minimum curvature algorithm to the gridded dataset for interpolating values between data points.

Conclusion

A new model of the basin configuration of Yucca Flat was created using the modified method of Jachens and Moring (1990). The model used gravity data which were edited to remove anomalous stations, incorporated well control data, and used an improved density-depth function. The resulting model conforms very well to existing geologic constraints and gives additional information about the *basement gravity*, and therefore, the geologic character of the basement beneath Yucca Flat.

The model can be improved further by comparing it to geologic data and interpretations (such as cross-sections) and by incorporating additional geophysical data (such as seismic and aeromagnetic data). The improved model will shed light on the *basement gravity*, which will in turn constrain basement geology. Information about the basement lithology penetrated in drill holes will provide guidance in interpreting the *basement gravity* field.

Acknowledgments

Work for this project was funded by the Department of Energy's (DOE) Environmental Restoration Program, Las Vegas. The authors would like to thank DOE for supporting this research. Special thanks to John Ferguson for sharing reprints and extensive notes on his earlier study. Thanks to Gary Dixon, Pete Rowley and Gayle Pawloski for data and guidance. Special thanks also to Donald Singer and Manual Nathenson for help in analyzing the borehole gravity information, to Ronald Wahl for sharing digital datasets, to the reviewers for helpful comments, and to all the others who generously shared data and ideas.

References

Blakely, Richard J., and Simpson, Robert W., 1986, Approximating edges of source bodies from magnetic or gravity anomalies: Geophysics, v. 51 no. 7, p. 1,494-1,498.

Cleveland, W.S., 1993: Visualizing Data. Summit, NJ: Hobart Press

Cole, James C., 1987, Breakup of an allochthonous slab: origin of the Yucca Flat Basin, Nevada Test Site: Geological Society of America Abstracts with Programs, v. 19, n. 7, p. 623.

Cole, J.C., Harris, A.G., Lanphere, M.A., and Barker, C.E., 1993, The case for pre-middle cretaceous extensional faulting in northern Yucca Flat, southwestern Nevada: Geological Society of America Abstracts with Programs, v. 25 n. 5, p. 22.

Ferguson, J. F., Felch, R. N., Aiken, C. L.V., Oldow, J. S., and Dockery, Holly, 1988, Models of the bouguer gravity and geologic structure at Yucca Flat, Nevada: Geophysics, v. 53, n. 2, p. 231.

Healey, D.L., 1966, Gravity and seismic study of Yucca Flat, Nevada Test Site, Nye County, Nevada in Harrison, D.A., and others, eds., Mining Geophysics: Society of Exploration Geophysicists Case Studies, v. 1, p. 84-93.

Healey, D.L., 1967a, Borehole gravity meter observations in drill hole UE19n, Pahute Mesa, Nevada Test Site: U.S. Geological Survey Technical Letter: Special Studies I-55, 11 p.

Healey, D.L., 1967b, Borehole gravity meter observations in drill hole UCe-18, Hot Creek Valley, Nye County, Nevada: U.S. Geological Survey Technical Letter: Central Nevada-11, 11 p.

Healey, D.L., 1968, Application of gravity data to geologic problems at Nevada Test Site: Geological Society of America Memoir 110, p. 147-156.

Healey, D.L., Clutsom, F.G., and Glover, D.A., 1984, Borehole gravity meter surveys in drill holes USW G-3, UE-25p#1, and UE-25c#1, Yucca Mountain area, Nevada: U.S. Geological Survey Open-File Report 84-672, 16 p.

Healey, D.L., Clutsom, F.G., and Glover, D.A., 1986, Borehole gravity meter surveys in drill hole USW G-4, Yucca Mountain Area, Nye County, Nevada: U.S. Geological Survey Open-File Report 86-205, 18 p.

Hinrichs, E.Neal, 1968, Geologic structure of the Yucca Flat area, Nevada: Geological Society of America Memoir 110, p. 239-246.

International Union of Geodesy and Geophysics, 1971, Geodetic Reference System 1967: International Association of Geodesy Special Publication no. 3, 116 p.

Jachens, R.C., and Moring, B.C., 1990, Maps of the thickness of Cenozoic deposits and the isostatic residual gravity over basement for Nevada: U.S. Geological Survey Open-File Report 90-404, 15 p., 2 plates, scale 1:1,000,000.

Jachens, Robert C., and Griscom, Andrew, 1985, An isostatic residual gravity map of California -- A residual map for interpretation of anomalies from intracrustal sources: in Hinze, W.J. ed., The utility of regional gravity and magnetic anomaly maps: Society of Exploration Geophysics, Tulsa, Oklahoma, p. 347-360.

Klima, James S., 1990, Simultaneous forward modeling of surface and borehole gravity from data from Yucca Flat, Nevada: m.s. Thesis, Colorado School of Mines, Golden, Colo., 153p.

Kososki, Bruce A., Robbins, Stephen L., and Schmoker, James W., 1987, Principal facts for borehole gravity stations in test well Ue19z, exploratory drill hole PM-1, and water well 5a, Nevada Test Site, Nye County, Nevada: U.S. Geological Survey Open-File Report 78-983, 16 p.

Plouff, Donald, 1977, Preliminary documentation for a FORTRAN program to compute gravity terrain corrections based on topography digitized on a geographic grid: U.S. Geological Survey Open-File Report 77-535, 45 p.

Ponce, D.A., 1997, Gravity data of Nevada: U.S. Geological Survey Digital Data Series DDS-42, CD-ROM.

Morelli, C. (Ed.), 1974, The International Gravity Standardization Net, 1971: International Association of Geodesy Special Publication no. 4, 194 p.

Robbins, S.L., Schmoker, J. W., and Hester, T.C., 1982, Principal facts and density estimates for borehole gravity stations in exploratory wells Ue4ah, Ue7j, Ue1h, Ue1q, Ue2co, and USW-H1 at the Nevada Test Site, Nye County, Nevada,: U.S. Geological Survey Open-File Report 82-277, 33 p.

Robbins, S.L., and Clutsom, F.G., 1983, Principal facts and density estimates for borehole gravity stations in exploratory wells Ue7h, Ue4al, and Ue11a at the Nevada Test Site, Nye County, Nevada,: U.S. Geological Survey Open-File Report 83-244, 20 p.

Schmoker, James W., and Kososki, Bruce A., 1978, Principal facts for borehole gravity stations in test wells Ue10j, Ue7ns, and Ue5n, Nevada Test Site, Nye County, Nevada: U.S. Geological Survey Open-File Report 78-212, 5 p.

Wahl, Ronald R., Sawyer, David A., Minor, Scott A., Carr, Michael D., Cole, James C., Swadley, W.C., Laczniak, Randell J., Warren, Richard G., Green, Katryn S., and Engle, Colin M., 1997, Digital geologic map database of the Nevada Test Site area, Nevada: U.S. Geological Survey Open-File Report 97-140 Rev. 3, 47 p.

Webring, Michael, 1981, MINC: A gridding program based on minimum curvature: U.S. Geological Survey Open-File Report 81-1224, 41 p.

Appendix

The digital data and text of this open file report is available from the following USGS URL: http://wrgis.wr.usgs.gov/open-file/of99-310/

Data Contents

The digital dataset consists of three files: points representing the depth to basement as defined in the text, lines representing the boundary of Yucca Flat as defined in this study, and points deleted from the original gravity dataset prior to creating the depth to basement model.

The file containing points of depth to basement is an ASCII data file, with one point coded per line. The points represent the center of 200m square grid cells when converted to UTM zone 11 NAD27 projection, and cover an area roughly 15' longitude by 15' latitude. The x-y locations of the points have been converted to standard geographic coordinates (decimal degrees). The depth values are accurate only within Yucca Flat. Because the dataset is based on a rectangular grid some data points exist outside of the valley boundary. These points should be considered inaccurate and ignored.

The file containing the boundary for Yucca Flat is an ASCII data file with the vertices for each line bracketed by the line ID and the key word END. The boundary was created by examining the break in slope for Yucca Flat, generalizing (smoothing) the boundary, and arbitrarily truncating the boundary in the narrow canyons which extend away from the valley.

The file containing points of deleted gravity values is an ASCII data file, with one point coded per line. The points are points which were removed by hand from the original gravity dataset due to their anomalous nature, as explained in the text. They are included here for completeness, and to ensure that our results are repeatable.

depth200.asc ASCII data file of depth to basement, coded as follows:
longitude,latitude,depth
Longitude and latitude are in decimal degrees, depth is
in meters.

boundary.asc ASCII data file of the boundary of Yucca Flat, as defined in this study, coded as follows:

```
id, longitude,
   longitude,latitude
   longitude,latitude
   longitude,latitude
   etc.
END
id, longitude,latitude
etc.
```

The id is an arbitrary line identifier. The longitude and latitude are in decimal degrees and represent the vertices of the line. The end of each line is defined by the word END.

del_data.asc ASCII data file of the location and value, in mgals, of the deleted gravity stations, coded as follows:

```
longitude,latitude,value
```

Longitude and latitude are in decimal degrees, depth is in meters.